Int. J. Solids Structures, 1969, Vol. 5, pp. 533 to 548. Pergamon Press. Printed in Great Britain

THE STRAIN RATE BEHAVIOR OF IRON IN PURE SHEAR*

JANUSZ KLEPACZKO†

Institute of Fundamental Technical Research
Polish Academy of Sciences, Warsaw, Poland

Abstract—An experimental study of the strain rate behavior of technically pure iron in pure shear is reported in this work. As is well known, most experimental results have been obtained from tension or compression tests; few results on strain rate behavior in pure shear.

Furthermore, dynamic tests on thin tubular specimens show several advantages over tension or compression tests.

Neglecting strain rate history effects the surface $\tau = \tau(\phi, \eta)$ has been experimentally obtained, where τ is the shear stress, ϕ and η are the shear strain and strain rate respectively. This surface was obtained over the following ranges of strain and strain rate $0 \leq \phi \leq 0{\cdot}42$; $1 \times 10^{-5}\ \text{sec}^{-1} \leq \eta \leq 1 \times 10^{2}\ \text{sec}^{-1}$.

In addition, a comparison between the effect of strain rate in pure shear, tension and compression tests has been carried out. This comparison enables preliminary data on the strain rate behavior in biaxial states of stress to be obtained.

Finally, the basic assumptions of the visco–plasticity theory for complex states of stress have been examined in the light of this experimental evidence.

1. INTRODUCTION

MUCH experimental work has been published to support the idea that iron and mild steel are extremely rate sensitive materials. However, the majority of these results have been obtained from tension or compression tests, and there are few results from pure shear tests. Experiments performed under conditions of pure shear can take the form of torsional tests on thin tubular specimens. This type of experiment has been reported, for example, by Klepaczko [7] on an investigation of strain rate effects in aluminum, and also in the work of Bennet and Sinclair [1] on the investigation of lower and upper yield limits as a function of loading time and temperature.

Dynamical investigations using thin tubular torsional specimens avoid many of the difficulties which are characteristic of tension or compression tests. In torsional tests there are no lateral inertia effects. It is well known that lateral inertia effects may produce, for example, a certain amount of error in the interpretation of strain hardening curves in the split Hopkinson pressure bar technique. Also, in torsional tests the cross section of a deformed specimen is constant, and the recorded strain hardening curve is at once in true coordinates, i.e. true stress vs. true strain.

On the other hand, the shear stress, τ, and the shear strain, γ, play an important role in all yield conditions for complex stress systems. Since rate dependence has been introduced into certain plasticity conditions, the investigation of the dynamic plastic behavior in pure shear is very important.

* Presented at the 12th International Congress of Applied Mechanics, Stanford, California, August 26–31, 1968.

† Now Visiting Scholar at the University of California, Department of Mineral Technology, Berkeley, California.

In addition, comparison of dynamic strain hardening curves obtained from pure shear tests with those obtained from tension or compression provide preliminary data on strain rate dependence for complex stress systems.

The aim of this work was to investigate the strain rate sensitivity of technically pure iron over the widest possible range of strain rates, and to compare the results with existing theories describing this phenomenon.

2. EXPERIMENTAL TECHNIQUE

All experiments were performed using thin tubular specimens with the following dimensions: outer diameter of the tubular part $D = 13$ mm, the length of this part $l_0 = 10$ mm, and wall thickness $y = 0{\cdot}5$ mm. Specimens were machined from technically pure iron of 0·05% carbon content. After machining, all specimens were annealed in a vacuum furnace for 2 hr at 850°C. Specimens prepared in this manner were twisted at different strain rates by means of a special torsional testing machine. This machine has been used in investigations over a lower strain rate γ. For the highest strain rates (of the order of $1 \times 10^2\ \text{sec}^{-1}$), a new device for the dynamical torsional tests was used. This device has been described by Klepaczko [6]. The torsional testing machine, as well as the dynamic testing arrangement, were equipped with suitable measuring devices for continuous recording of the torque and the angle of twist as functions of time.

Strain hardening curves relating shear stress, τ, to the shear strain, ϕ (where ϕ is obtained from $\phi = \tan\gamma$, γ being the angle of shear strain), were obtained from oscillograph records, taken at different strain rates $\eta = \mathrm{d}\phi/\mathrm{d}t$. In the present investigation, the following magnitudes of strain rate η were used: $\eta_1 = 1{\cdot}17 \times 10^{-5}\ \text{sec}^{-1}$; $\eta_2 = 1{\cdot}31 \times 10^{-4}\ \text{sec}^{-1}$; $\eta_3 = 2{\cdot}77 \times 10^{-3}\ \text{sec}^{-1}$; $\eta_4 = 2{\cdot}85 \times 10^{-2}\ \text{sec}^{-1}$; $\eta_5 = 4{\cdot}4 \times 10^{-1}\ \text{sec}^{-1}$, and for the dynamical testing arrangement $\eta_{\max} \simeq 55\ \text{sec}^{-1}$. The ratio of the highest strain rate to the lowest one reaches the value

$$x = \frac{\eta_{\max}}{\eta_1}, \qquad x = 4{\cdot}7 \times 10^6.$$

For each of the six values of strain rate given above, three or four tests were performed and the strain hardening curves for each strain rate were obtained by averaging.

3. EXPERIMENTAL RESULTS AND DISCUSSION

In general, attempts to describe the rate dependent behavior of metals have used data obtained at constant or nearly constant strain rates. Thus, in constitutive equations so obtained the strain rate is treated as an independent variable, while in tests it is a parameter. Since it neglects strain rate history effects, this type of mathematical description of strain rate behavior may be treated as a first approach. A number of strain rate history effects for mild steel and aluminum have been discussed in the works of Klepaczko [8], and also [7] and [9].

In the remainder of this work strain rate history effects will be neglected, and all interpretations of experimental results will be performed from this point of view.

Several averaged strain hardening curves $\tau = \tau(\phi, \eta)$, η = constant, for different strain rates have been obtained; these curves are shown in Fig. 1, which clearly indicates that the iron investigated here is extremely rate sensitive. The intensive strain rate dependence is

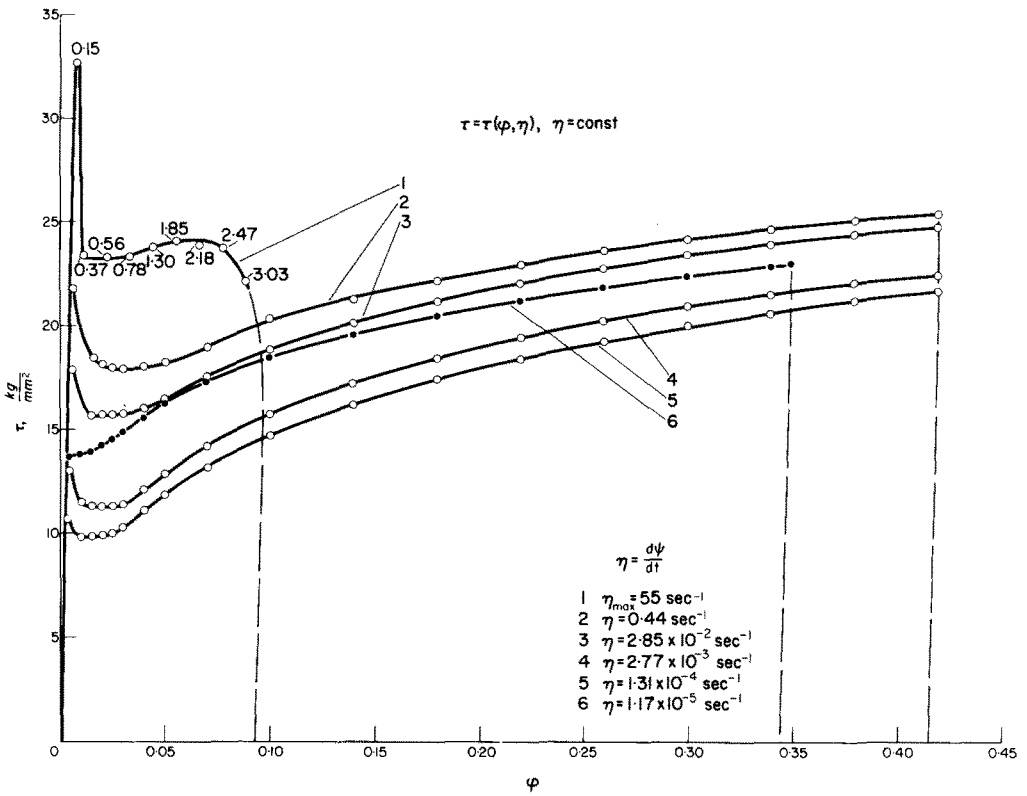

FIG. 1. Averaged strain hardening curves $\tau = \tau(\phi, \eta)$, η = const., obtained in pure shear. Numbers at the points of curve 1, $\eta_{max} \simeq 55\,\text{sec}^{-1}$, denote time in msec.

noted for upper yield limits, and stress differences between upper and lower yield points decrease as the strain rates decrease. At the value of strain rate $\eta = 1{\cdot}17 \times 10^{-5}\,\text{sec}^{-1}$ the upper yield limit disappears completely, but the entire strain hardening curve is higher than the two curves obtained at two higher strain rates, namely for $\eta = 1{\cdot}31 \times 10^{-4}\,\text{sec}^{-1}$ and $\eta = 2{\cdot}77 \times 10^{-3}\,\text{sec}^{-1}$. For this reason the strain hardening curve of the lowest strain rate has been denoted in Fig. 1 by the black points. It is interesting to note that the curve obtained at the lowest strain rate shows a lower strain hardening rate $\partial\tau/\partial\phi$ than the other curves. Due to this fact specimens tested at the lowest strain rate lost stability earlier (at lower strains) than is observed for higher strain rates.

As has been mentioned, strain hardening curves obtained in this manner constitute a surface $\tau = \tau(\phi, \eta)$; of course, in this case the strain rate history effects are neglected. Cross sections of the surface $\tau = \tau(\phi, \eta)$ obtained for different values of strain, ϕ = constant are shown in Fig. 2. The black circles denote stresses at the upper yield points, $\tau_0 = \tau_0(\eta)$,

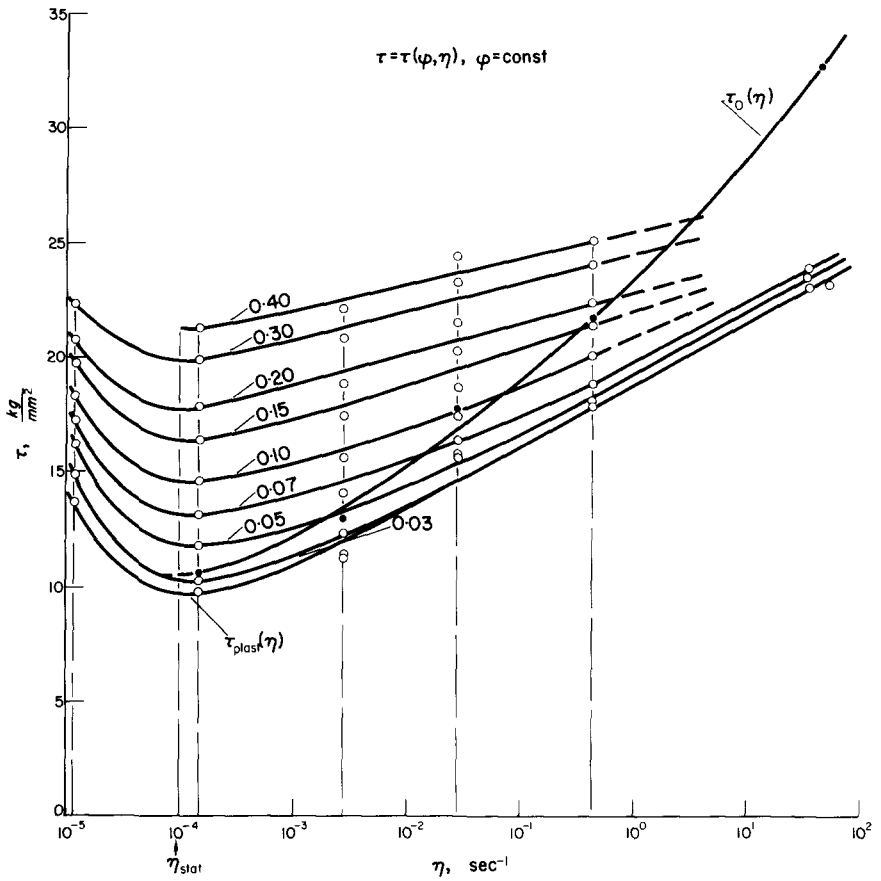

FIG. 2. Cross sections of the surface $\tau = \tau(\phi, \eta)$ obtained for different values of strain. The vertical dashed lines denote values of applied strain rates.

and the cross section at the lower yield limit is denoted by $\tau_{pl} = \tau_{pl}(\eta)$. The spreading of points indicates that the average strain hardening curve for $\eta = 2{\cdot}77 \times 10^{-3}\ \text{sec}^{-1}$ should be a little higher, about 0·6 kg/mm^2, and the curve for $\eta = 2{\cdot}85 \times 10^{-2}\ \text{sec}^{-1}$ a little lower, about 0·8 kg/mm^2. The strain hardening curve for $\eta_{\max} = 55\ \text{sec}^{-1}$ has not been obtained at exactly constant strain rate, and for this reason the points of this curve do not lie in one section $\eta = \text{constant}$.

It is interesting to note that the minimum of the flow stress appears near the strain rate region of $\eta \simeq 1 \times 10^{-4}\ \text{sec}^{-1}$. This value of strain rate is commonly accepted as the "statical" one. A similar minimum has been experimentally observed many times, but usually for higher strain rates and higher temperatures. For example, Manjoine [14] reported such a minimum for a mild steel at a strain rate in tension of $\dot{\varepsilon} = 1\ \text{sec}^{-1}$ at temperature $t = 200°\text{C}$; however, for $t = 400°\text{C}$ this minimum was observed for $\dot{\varepsilon} = 3 \times 10^2\ \text{sec}^{-1}$. Recently, this phenomenon has been discussed by Tanaka and Kinoshita [22]. Investigations by these authors have shown that decreasing temperature involves a displacement of this minimum into the region of lower strain rates. The appearance of such a minimum observed in this work at the strain rate $\eta \simeq 1 \times 10^{-4}\ \text{sec}^{-1}$ can be so explained. This value

of strain rate, i.e. $\eta = 1 \times 10^{-4}\,\text{sec}^{-1}$ is equivalent to the value for tension or compression, $\dot{\varepsilon} = 5{\cdot}76 \times 10^{-5}\,\text{sec}^{-1}$, where $\dot{\varepsilon} = \eta/\sqrt{3}$.

From the point of view of the physical mechanisms of plastic deformation this displacement of the flow stress minimum suggests that the structural changes accompanying plastic deformation are to some extent equivalent at different temperatures, and strain rates respectively. Such an effect is generally believed to be connected with diffusion processes which take place during plastic deformation, referred to as strain aging.

The experimentally obtained surface $\tau = \tau(\phi, \eta)$ is shown in stereographic projection in Fig. 3, over the strain range $0 \leq \phi \leq 0{\cdot}42$, and within the strain rate limits $1 \times 10^{-5}\,\text{sec}^{-1} \leq \eta \leq 1 \times 10^{2}\,\text{sec}^{-1}$. In the basal plane (ϕ, η) the strain rate histories

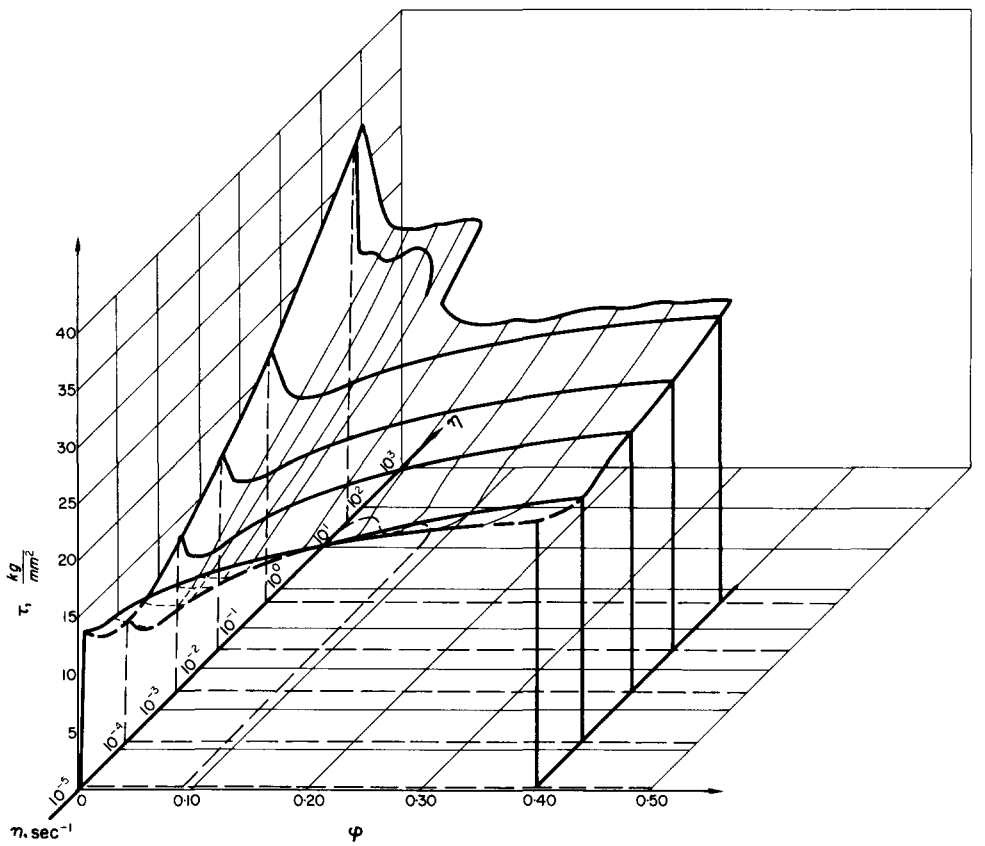

FIG. 3. Stereographic projection of the surface $\tau = \tau(\phi, \eta)$. The dashed lines on the (ϕ, η) plane show the strain rate histories $\eta = \eta(\phi)$.

$\eta = \eta(\phi)$ for each strain hardening curve have been marked by dotted lines. Such surfaces have been given previously by Krafft [10], and Krafft and Sullivan [11] for the strain rate $1\,\text{sec}^{-1} \leq \dot{\varepsilon} \leq 3{\cdot}10^{2}\,\text{sec}^{-1}$ and strain $0 \leq \varepsilon \leq 0{\cdot}08$ ranges, also by Murch and Campbell [15] for $1 \times 10^{-4}\,\text{sec}^{-1} \leq \dot{\varepsilon} \leq 10\,\text{sec}^{-1}$, and $0 \leq \varepsilon \leq 0{\cdot}05$. However, all these surfaces were obtained for mild steels of $\sim 0{\cdot}20\%$ C [10], [11], and $\sim 0{\cdot}085\%$ C in reference [15], and both for compression tests.

It should be stressed that the surface shown in Fig. 3 is obtained under pure shear conditions for technically pure iron of ~0·05% C. Due to the lack of experimental results describing such a surface for technically pure iron (~0·05% C) under tension or compression for the same range of strains and strain rates as in the present work, it is impossible to compare strain rate behavior for these two stress systems over the entire range of strain and strain rate. Fortunately, this comparison can be done for upper and lower yield limits.

A basis for this comparison is the Huber–Mises yield condition, namely

$$\sigma = \sqrt{3}\tau; \qquad \varepsilon = \frac{\phi}{\sqrt{3}}; \qquad \dot{\varepsilon} = \frac{\eta}{\sqrt{3}} \tag{1}$$

The results of this comparison have been plotted in logarithmic coordinates and shown in Fig. 4. The data of the following authors are used: Schofman [19], March and Campbell [15]; Tanaka *et al.* [21], and finally Winlock [23]. The dashed lines refer to upper yield limits, and the solid lines refer to lower ones. The present results suitably modified by use of (1) are included.

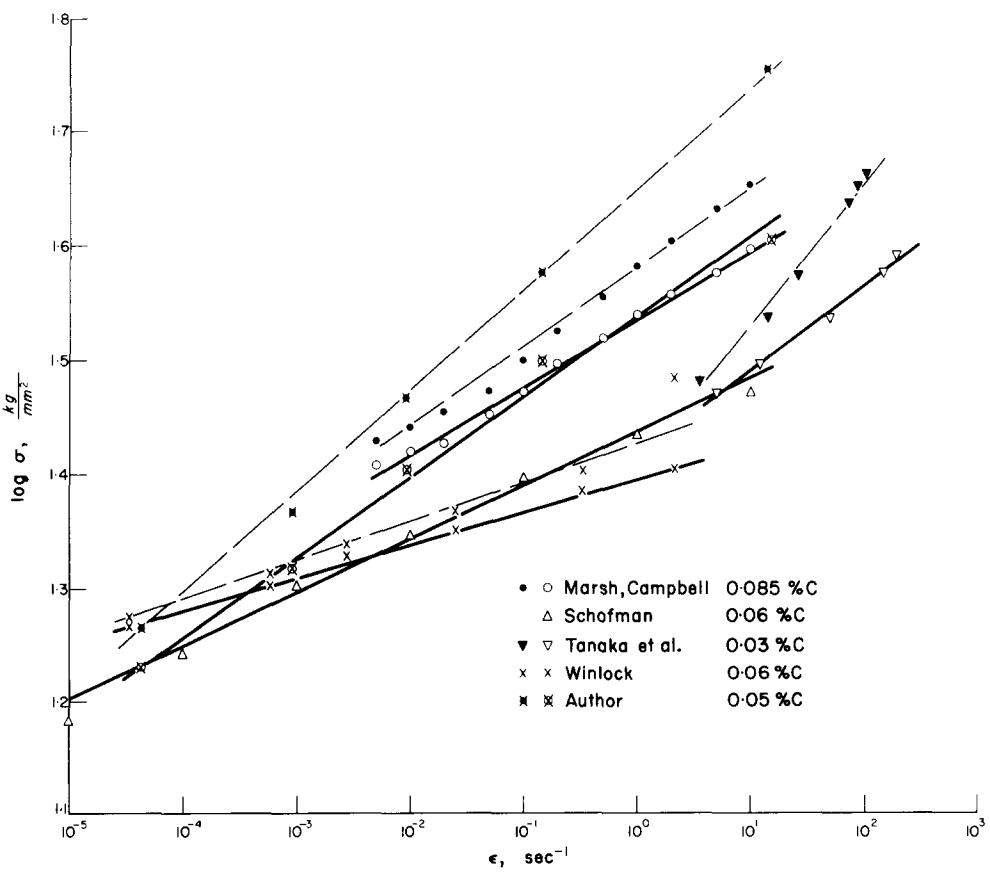

FIG. 4. Comparison of the upper and lower yield limits according to different references along with the present results. The solid lines denote lower yield point stress at the $\sigma_p I(\varepsilon)$, the dashed lines denote upper yield stresses, the thick lines represent results from the pure shear experiments.

The first conclusion which is immediately visible from Fig. 4, is that the strain rate behavior of upper and lower yield limits are ascribable quantitatively by a definition of strain rate sensitivity n of the form

$$n = \frac{\partial \log \sigma}{\partial \log \dot{\varepsilon}} \tag{2}$$

In terms of the double logarithmic scale, the strain rate sensitivity n is represented simply as the slope of the experimentally obtained straight lines. It is remarkable that the strain rate sensitivity definition n remains independent of stress system, i.e. is independent of the condition of plasticity. If n remains constant for increasing strain rates, then for upper and lower yield limits one can obtain respectively

$$\sigma_0 = C_1 \dot{\eta}^{n_0} \quad \text{and} \quad \sigma_{pl} = C_2 \dot{\eta}^{n_{pl}} \tag{3}$$

All data obtained for n_0 and n_{pl} from all sources (for the strain rate range $4 \times 10^{-5}\ \text{sec}^{-1} \leq \dot{\varepsilon} \leq 10^{2}\ \text{sec}^{-1}$) have been tabulated in Table 1.

TABLE 1

Source	Authors	%C	Kind of experiment	n_0	n_{pl}
[15]	Marsh and Campbell (1963)	0·085	Compression (hydraulic machine)	0·0697	0·0593
[19]	Schofman (1964)	0·06	Tension		0·0487
[21]	Tanaka *et al.* (1966)	0·03	Compression (modified Hopkinson pressure bar)	0·1240	0·0740
[23]	Winlock (1953)	0·06	Tension	0·0343	0·0288
	Present work	0·05	Torsion of tubular specimens	0·0877	0·0702

Results shown in Fig. 1 and Table 1 indicate that a comparison between data from this work and that of other authors could be done using the results obtained by Schofman [19], and Winlock [23]. This suggestion arises from the fact of essentially equal lower yield limits for data mentioned at the strain rate value of $\dot{\varepsilon} \simeq 1 \times 10^{-4}\ \text{sec}^{-1}$. Also, the carbon content is of the same order.

The Murch and Campbell results were obtained for a mild steel of 0·085% carbon content, for which the equivalent points lie somewhat higher, i.e. higher yield stresses. Results reported by Tanaka and others have been obtained by means of a split Hopkinson pressure bar technique, and for somewhat higher strain rates. Since, as it is well known, the lateral inertia effects and the specimen face friction may lead to an apparent increase of the strain rate sensitivity, so the values of n obtained may be higher than expected.

In the light of this comparison the conclusion which may be deduced is that the upper and lower flow limits show higher strain rate sensitivity in the case of pure shear than for tension and compression tests.

This conclusion is confirmed in the work by Lindholm and Yeakley [12] where the strain rate sensitivity of a mild steel was investigated using simultaneous torsion and tension, and only torsion or tension.

Since the increase of the upper yield limit can be approximated by the formula

$$\tau_0 = C_1^* \eta^{n_0}, \qquad 1 \times 10^{-4}\,\text{sec}^{-1} \leq \eta \leq 10^2\,\text{sec}^{-1} \tag{4}$$

where n_0 is the strain rate sensitivity for the upper yield limit and C_1^* is a material constant, the delay time t_d may be easily evaluated. It is noted that in the case of pure shear, C_1^* depends on C_1 from equation (4) according to the relation

$$C_1^* = 3^{-(1+n_0)/2} C_1$$

For the purpose of evaluation of delay time t_d, it was assumed that during loading the average strain rate $\bar{\eta}$ is constant, for this case

$$\phi_0 = t_d \bar{\eta},$$

also, Hooke's law holds

$$\tau_0 = G\phi_0,$$

where G is the shear modulus.

Taking into account the above relationships the delay time can be calculated in the form

$$t_d = \left(\frac{C}{\tau_0}\right)^{\alpha} \quad \text{for} \quad t_d \leq t_c \tag{5}$$

or

$$\tau_0 = \frac{C}{t^{1/\alpha}} \tag{6}$$

where

$$\alpha = \frac{1}{n_0} - 1, \qquad C = \left(\frac{C_1^*}{G^{n_0}}\right)^{1/(1-n_0)}$$

If t_c is the time when the static upper yield point is reached at the strain rate $\eta_{\text{stat}} = 1 \times 10^{-4}\,\text{sec}^{-1}$, then

$$t_c = \phi_0 \times 10^4\,[\text{sec}], \quad \text{or} \quad t_c = \frac{\tau_0}{G} 10^4\,[\text{sec}].$$

Assuming a shear modulus $G = 8{\cdot}1 \times 10^3\,\text{kg/mm}^2$ and using the experimental data the upper yield point stress for $\eta = 1 \times 10^{-4}\,\text{sec}^{-1}$ which is $\tau_0 = 10{\cdot}6\,\text{kg/mm}^2$, the time t_c becomes $t_c \simeq 13{\cdot}1$ sec. Simultaneously, C_1 and n_0 are also known from the experiments, (see Fig. 4, $C_1 = 43{\cdot}95\,\text{kg/mm}$, $n_0 = 0{\cdot}0877$) and hence the constants C_1^*, C and α are $C_1^* = 24{\cdot}2\,\text{kg/mm}^2$, $C = 13{\cdot}83\,\text{kg/mm}^2$, $\alpha = 10{\cdot}4$. Thus, in the double logarithmic scale, $\log \tau_0$ vs. $\log t_d$, the relationship (5) becomes a straight line with negative slope, crossing the horizontal line $\log \tau_0 = \text{const}$ at the point $\tau_0 = 10{\cdot}6\,\text{kg/mm}^2$ for $t_c = 13{\cdot}1$ sec.

Usually, the relationship between stress and delay time is plotted with a linear stress scale and time logarithmic. These two descriptions differ insignificantly.

A more exact comparision of these experimental results with other delay time data could be carried out, using, for example, the review by Goldsmith [2].

4. AN ANALYSIS OF ASSUMPTIONS USED IN THE CONTINUUM THEORY OF PLASTICITY

Previous efforts to theoretically describe the dynamic plastic behavior of metals may be divided into two categories. The first is an increasingly exact mathematical description of the one dimensional case, using mostly a phenomenological approach. This approach is closely connected with the phenomenon of elasto-plastic stress wave propagation in bars. The second approach is connected with a generalization of complex stress system descriptions. However, in this case the assumptions which are usually made considerably accede experimental observations. Both approaches will be briefly discussed below.

At present, the most frequently used constitutive relation, for which the mechanical equation of state concept is assumed, may be called the Malvern–Sokolovsky equation, [13] and [20],

$$E\dot{\varepsilon} = \dot{\sigma} + g(\sigma, \varepsilon) \tag{7}$$

When the $\sigma - f(\varepsilon)$ argument is introduced, the g-function takes the following form

$$\dot{\varepsilon}_p = g_M[\sigma - f(\varepsilon)] \quad \text{or} \quad \dot{\varepsilon} = \frac{\dot{\sigma}}{E} + g_M[\sigma - f(\varepsilon)], \tag{8}$$

where $f(\varepsilon)$ denotes a "static" strain hardening curve, usually obtained at the "statical" strain rate $\dot{\varepsilon} \simeq 1 \times 10^{-4}\,\text{sec}^{-1}$, g_M is an unspecified function of $[\sigma - f(\varepsilon)]$ obtainable from experimental data. Equation (8) in the more convenient inverse form is

$$\sigma = f(\varepsilon) + g_M^{-1}(\dot{\varepsilon}). \tag{9}$$

Depending on the problem under consideration, different g_M-functions are used, for example, the following one is frequently assumed

$$\dot{\varepsilon} = \frac{\dot{\sigma}}{E} + \gamma_1 g_{M^1}[\sigma - f(\varepsilon)], \tag{10}$$

where γ_1 is a material constant.

The Malvern–Sokolovsky equation, in a more simple case, i.e. the linear one,

$$\dot{\varepsilon} = \frac{\dot{\sigma}}{E} + \gamma_1[\sigma - f(\varepsilon)]$$

has been recently generalized in the work of Kelly [5], by its treatment as a functional of the strain and strain rate, in which the delayed yield phenomenon was also taken into consideration.

The first approach describing the rate-sensitive behavior of a material in complex states of stress is reported in the work of Hohenemser and Prager [3]. This generalization has been performed for the Bingham model. Using this basis and the Malvern–Sokolovsky equation, further generalizations of the theory were given by Perzyna [16] and [17], taking also into consideration the strain hardening phenomenon. The proposed relations have the form

$$\dot{e}_{ij} = \frac{1}{2\mu}\dot{s}_{ij} + \gamma\langle\Phi(F)\rangle\frac{s_{ij}}{\sqrt{(J_2)}}, \qquad \dot{\varepsilon}_{ii} = \frac{1}{3K}\dot{\sigma}_{ii}, \tag{11}$$

where e_{ij} and s_{ij} denote deviators of strain and stress respectively, μ and K are elastic constants, γ is a material constant, and

$$\langle \Phi(F) \rangle = \begin{cases} 0 & \text{for} \quad F \leq 0 \\ \Phi(F) & \text{for} \quad F > 0. \end{cases}$$

F plays the role of an argument

$$F = \frac{\sqrt{(J_2)}}{\kappa} - 1.$$

The κ represents a strain hardening parameter, which, for the one dimensional case, is identified with a "static" strain hardening curve. A little different definition of κ was introduced in the work of Kaliski [4]. The form of the function $\Phi(F)$ is usually chosen to be consistent with the real dynamic behavior of a particular metal.

For the one dimensional case, equation (11) can be reduced to

$$\dot{\varepsilon} = \frac{\dot{\sigma}}{E} + \frac{2\gamma}{\sqrt{3}} \left\langle \Phi \left[\frac{\sigma}{f(\varepsilon_p)} - 1 \right] \right\rangle \tag{12}$$

or

$$\dot{\varepsilon} = \frac{\dot{\sigma}}{E} + \frac{2}{\sqrt{3}} \gamma \langle \Phi(F) \rangle,$$

or inversely

$$\sigma = f(\varepsilon_p) \left[1 + \Phi^{-1} \left(\frac{\sqrt{(3)} \dot{\varepsilon}_p}{2\gamma} \right) \right] \tag{13}$$

Equation (14) shows an analogous shape as equation (10); it differs only due to the definition of the F parameter. In attempting to describe the real behavior of metals this difference involves different γ behavior than γl as a function of a strain.

All studies of strain rate behavior in complex stress systems have been made under the following assumptions:

(a) The Huber–Mises yield condition is satisfied,

(b) The isotropic strain hardening takes place at increasing strains,

(c) The influence of strain rate on yield condition is isotropic.

The existence of a higher strain rate sensitivity for pure shear than for tension or compression seems not to confirm the c assumption. As was mentioned earlier, the higher strain rate sensitivity in shear has been obtained by Lindholm and Yeakley [12]; this also supports the above conclusion.

In order to evaluate relationship (11) the experimental results of Fig. 1 and Fig. 2 have been used, and simultaneously the following $\Phi(F)$ function is assumed

$$\Phi(F) = F^{\delta}. \tag{14}$$

Thus, in pure shear

$$\eta = \gamma_* F^{\delta} \quad \text{or} \quad F = \beta \eta^{n_*},$$

and finally

$$\tau = \tau_{\text{stat}}(\phi)[1 + \beta \eta^{n_*}], \tag{15}$$

where $n_* = 1/\delta$, $\beta = 1/\gamma_*^{1/\delta}$. The material constant n_* is analogous to the strain rate sensitivity n according to equation (2).

Values of F as a function of strain ϕ, and strain rate η, from the formula $F = \beta\eta^{n*}$ have been shown in Fig. 5 and Fig. 6, using experimental data which were shown above. The "statical" strain rate is assumed to be $\eta_0 = 1 \times 10^{-4}$ sec^{-1}. It follows from Fig. 5 and Fig. 6 that the F argument depends very strongly upon strain rate as well as strain. The relationship (15) implies a straight line with slope n_* in the double logarithmic coordinates log F vs. log η. To evaluate this, using the experimental data, plots of log F against log η for different strain values have been made. The results for strains $\phi_0 \leq \phi \leq 0{\cdot}40$, and strain rates 1×10^{-3} sec$^{-1} \leq \eta \leq 1 \times 10^{2}$ sec^{-1} are shown in Fig. 7. The solid curves obtained from experimental data have been approximated by dashed straight lines for different strains according to the formula $F = \beta\eta^{n*}$. Further, for each value of strain ϕ, the values of β and n_* have been found; also, the equivalent material constants γ_* and δ were obtained. The results are shown in Table 2 and in Fig. 8.

These results lead to the conclusion that β is strongly dependent upon strain, while on the contrary n_* and δ can be, to some extent, recognized as material constants. The average values of n_* and δ are $\bar{n}_* = 0{\cdot}187$, and $\bar{\delta} = 5{\cdot}33$.

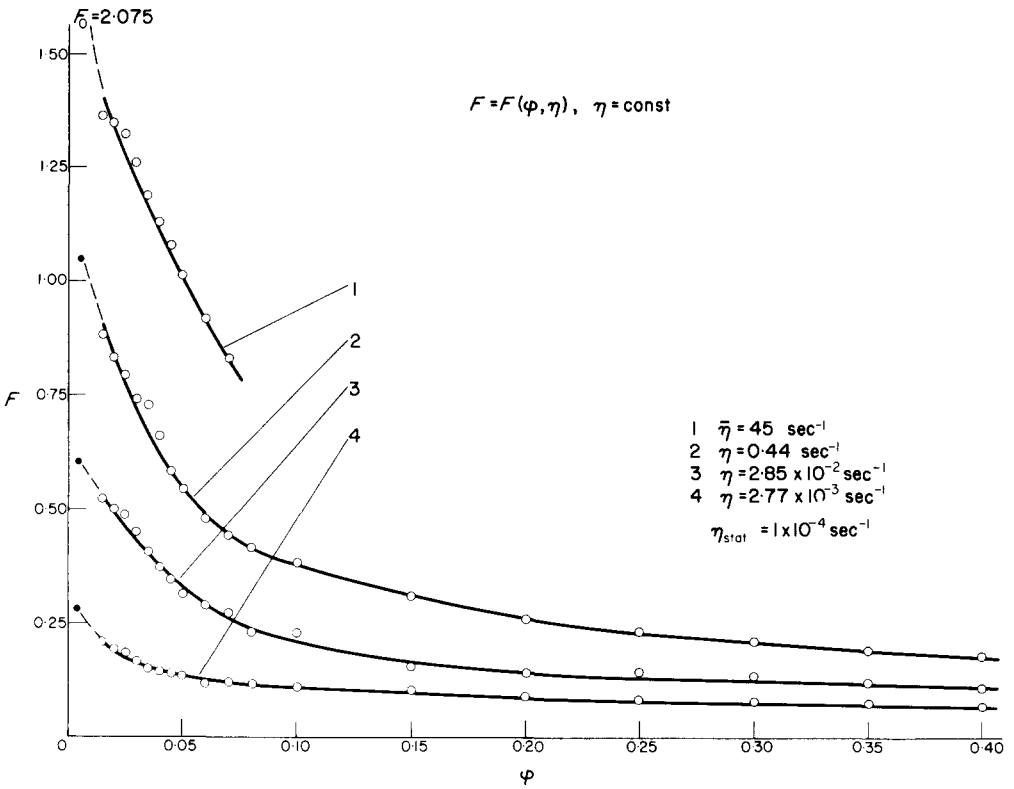

FIG. 5. Experimentally obtained values of the argument $F = \tau/\tau_{stat}(\phi) - 1$ for different strain rates, $\tau_{stat}(\phi)$ assumed at $\eta = 1 \times 10^{-4}$ sec^{-1}.

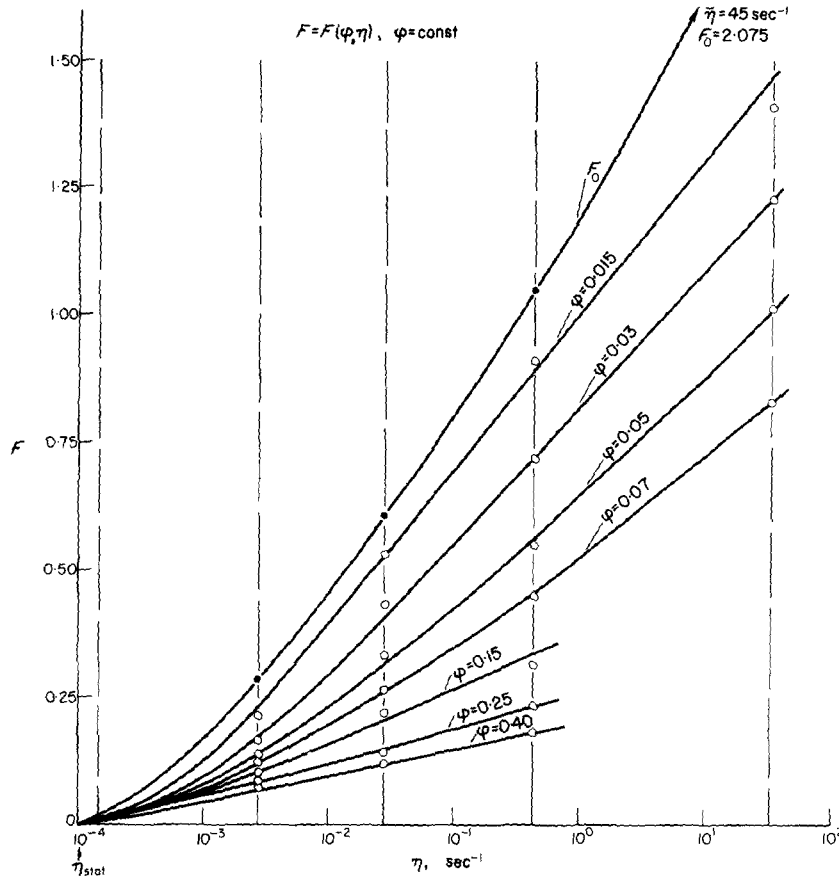

FIG. 6. Experimentally obtained values of the F-argument for different strains.

In order to accurately describe the strain rate behavior of technically pure iron by a relationship such as (14) and (15), the following modification for the one dimensional case could be introduced, namely

$$F = \beta(\phi)\dot{\eta}^{n*} \quad \text{or} \quad \dot{\eta} = \gamma_*(\phi)F^{\delta}. \tag{16}$$

Such a modification leads to the relationship

$$\tau = \tau_{stat}(\phi)[1 + \beta(\phi)\dot{\eta}^{n*}], \tag{17}$$

where $\beta(\phi)$ is a decreasing function of strain; this function, obtained on the basis of experimental data, is shown in Fig. 8. Thus the equation $F = \beta\dot{\eta}^{n*}$ is a good approximation to the strain rate behavior of the iron investigated only for constant values of strain.

It was ascertained above that the arguments of both equations (10) and (12) are different. This fact is not important for the ideal plastic and strain rate sensitive behavior model, but for the real behavior, when strain hardening takes place, this difference is a fundamental

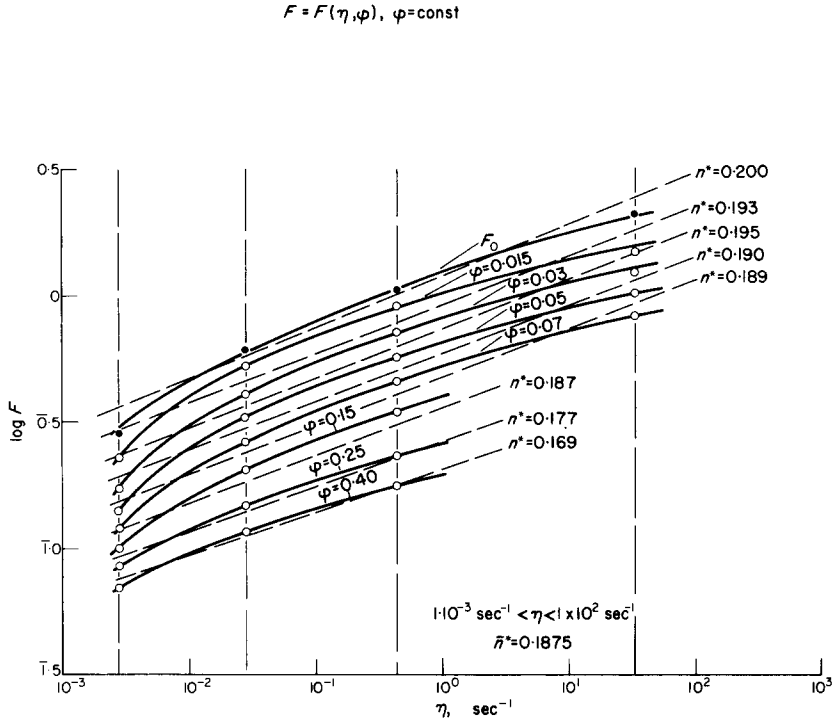

FIG. 7. Experimental values of the F-argument as a function of strain rate η, (shown in the double logarithmic scale for different values of strain ϕ). The dashed lines constitute successive descriptions by the relationship (17).

TABLE 2

ϕ	n_*	$\delta = \frac{1}{n_*}$	β	$\gamma_* \frac{1}{\beta^\delta}$
ϕ_0†	0·200	5·000	1.1780	0·4400
0·015	0·193	5·181	0·9074	1·654
0·03	0·195	5·128	0·7320	4·952
0·05	0·190	5·263	0·5857	16·70
0·07	0·189	5·291	0·4682	55·45
0·15	0·187	5·348	0·3595	237·7
0·25	0·177	5·650	0·2619	1940·0
0·40	0·169	5·917	0·2043	12060·0

† ϕ_0 denotes strain at the upper yield limit.

one. Then equation (10) leads to the relations

$$\sigma = f(\varepsilon)\left[1 + \frac{\beta_M}{f(\varepsilon)}\dot{\varepsilon}^{n_*}\right], \tag{18}$$

and simultaneously, equation (14) implies

$$\sigma = f(\varepsilon)[1 + \beta_p \dot{\varepsilon}^{n_*}], \tag{19}$$

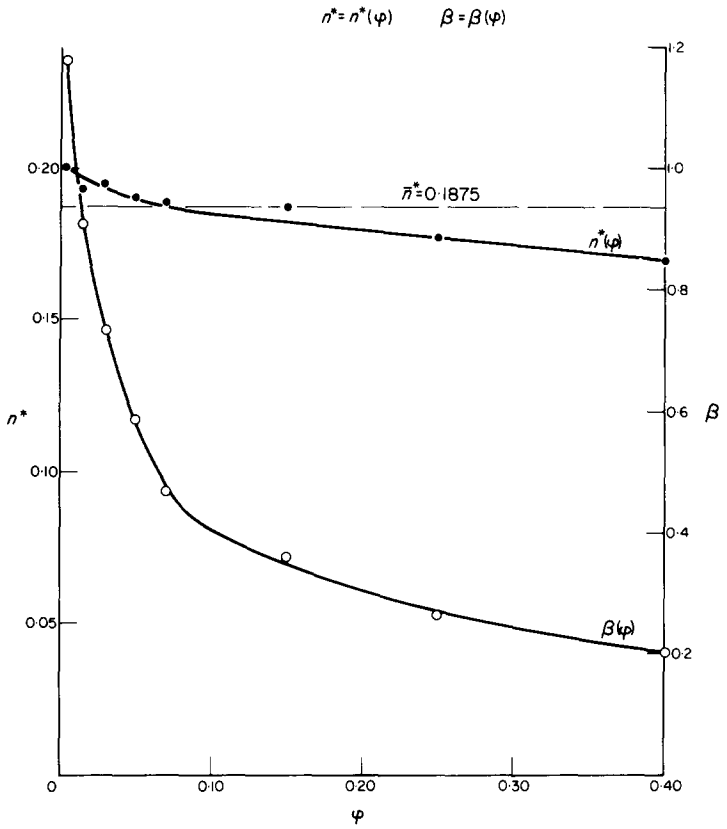

FIG. 8. Observed changes of β and n_* with increasing strains; the approximation used is $F = \beta\eta^{n^*}$.

thus

$$\beta_M = \beta_p f(\varepsilon).$$

Recalling that β_p is a sharply decreasing function of strain and at the same time the strain hardening curve $f(\varepsilon)$ is an increasing function of strain, β_M will be less likely to change with increasing strain. Thus it may be suggested, when strain hardening is taken into consideration, that a better approach is to use equation (8) with the argument $\sigma - f(\varepsilon)$, than equation (14) with $F = [\sigma - f(\varepsilon)]/f(\varepsilon)$. It also seems that the more reasonable description of the dynamic strain hardening curves for mild steel and iron can be achieved accepting the F parameter but using the strain rate sensitive and ideal plastic model instead of the analogous strain hardening model.

The analysis performed is not exhaustive, but provides a certain amount of information to explain the response of mild steel and iron to high strain rate deformation under conditions of complex stress. It is necessary to perform further experimental work for the purpose of verification of the assumptions which were introduced into the theory of viscoplasticity for complex stresses. A more extensive discussion of the theories and assumptions which must be verified has been carried out in the work of Perzyna [18].

5. CONCLUSIONS

The experimental results and analysis performed lead to the following conclusions:

(i) The torsional tests appear to be very useful for the investigation of strain hardening curves under dynamic conditions. During such a test there are no lateral inertia effects, and also the cross section of a deformed specimen remains constant. Thus, at once, the true strain hardening curve can be recorded.

(ii) For all values of strains, i.e. $\phi_0 \leq \phi \leq 0{\cdot}42$, the minimum flow stress has been experimentally observed, approximately at the strain rate $\eta \simeq 1 \times 10^{-4}\,\mathrm{sec}^{-1}$.

(iii) At the value of strain rate $\eta \simeq 1{\cdot}17 \times 10^{-5}\,\mathrm{sec}^{-1}$ the disappearance of upper yield point has been observed. For increasing strain rates, the increase of upper yield stress is more intensive than the lower yield stress.

(iv) These investigations have shown also that over the strain rate region $1 \times 10^{-4}\,\mathrm{sec}^{-1} \leq \eta \leq 1 \times 10^{2}\,\mathrm{sec}^{-1}$ the stresses of upper and lower yield limits can be well described by the strain rate sensitivity definition.

$$n = \frac{\partial \log \tau}{\partial \log \eta}.$$

(v) The comparison between strain rate behavior of technically pure iron obtained by different investigators in tension or compression with the present experimental results, obtained under conditions of pure shear, should lead to the conclusion that the iron is more strain rate sensitive in pure shear than for tension or compression. This conclusion implies also that the above assumption about isotropic strain rate sensitivity used in the theory of visco-plasticity does not seem to be exactly satisfied.

(vi) It seems reasonable, while the $\dot{\varepsilon} = \gamma\langle\phi(F)\rangle$ concept of strain rate description is used, to apply the model without considering strain hardening (the strain rate sensitive ideal plastic model) rather than to include strain hardening phenomenon.

Acknowledgement—A part of this work was done at the University of California, Berkeley, where the author stayed while supported by a Ford Foundation grant. Both sources are gratefully acknowledged.

REFERENCES

[1] P. E. Bennet and C. M. Sinclair, *J. bas. Engng* **83D**, 557 (1961).
[2] W. Goldsmith, *Impact*. Arnold (1960).
[3] K. Hohenemser and W. Prager, *Z. angew. Math. Mech.* **12**, 216 (1932).
[4] S. Kaliski, *Bull. Acad. pol. Sci. Ser. Sci. tech.* **11**, 239 (1963).
[5] J. M. Kelly, *Int. J. Solids Struct.* **3**, 521 (1967).
[6] J. Klepaczko, *Mechanika Teoretyczna i Stosowana* **5**, (1967).
[7] J. Klepaczko, *Archwm. Mech. stosow.* **19**, 211 (1967).
[8] J. Klepaczko, Doctoral Thesis, Institute of Fundamental Technical Research, Polish Academy of Sciences, Warsaw (1965).
[9] J. Klepaczko, *Mechanika Teoretyczna i Stosowana* **4**, 43 (1966).
[10] J. M. Krafft, *Response of Metals to High Velocity Deformation*. Interscience (1961).
[11] J. M. Krafft and A. M. Sullivan, *Trans. Am. Soc. Metals* **51**, 643 (1959).
[12] V. S. Lindholm and L. M. Yeakley, *Exp. Mech.* **7**, 1 (1967).
[13] L. E. Malvern, *J. appl. Mech.* **18**, 203 (1951).
[14] M. J. Manjoine, *J. appl. Mech.* **11**, 211 (1944).
[15] K. J. March and J. D. Campbell, *J. Mech. Phys. Solids* **11**, 49 (1963).
[16] P. Perzyna, *Q. appl. Math.* **20**, 321 (196).
[17] P. Perzyna, *Proc. Vibr. Probl.* **4**, 1 281 (1963).

[18] P. PERZYNA, *Adv. appl. Mech.* **9**, 243 (1966).
[19] L. A. SCHOFMAN, *Theory and Application of Metalworking Processes.* Moscow (1964).
[20] V. V. SOKOLOVSKY, *PMM* **12**, 261 (1948).
[21] K. TANAKA, T. MATSUO, M. KINOSHITA and T. MAEDE, *Bull. J.S.M.E.* **6**, 21 (1966).
[22] K. TANAKA and M. KINOSHITA, *Bull. J.S.M.E.* **10**, 429 (1967).
[23] J. WINLOCK, *Trans. Am. Inst. Min. metall. Engrs* **179**, 797 (1953).

(*Received* 18 *March* 1968; *revised* 31 *July* 1968)

Абстракт—В работе описывается экспериментальное исследование поведения скорости деформации технически чистого железа при чистом сдвиге. Как хорошо известно, большинство экспериментальных результатов получено из испытаний растяжения или сжатия, тогда как немного результатов на поведние скорости деформации ири чистом сдвиге.

Кроме того, динамические испытания на тонких трубчатых образцах указывают отдельные преимущества над исследованиями растяжения или сжатия.

Пренебрегая эффектами истории скорости деформации получается экспериментально поверхность $\tau = \tau(\phi, \eta)$, где τ обоэначает напряжение сдвига, ϕ и η являются соответственно деформацией сдвига и скоростью деформации. Определяется поверхность выше следующих пределов деформации и скорости деформации $0 \leqslant \phi \leqslant 0{,}42$: 1×10^{-5} сек$^{-1} \leqslant \eta \leqslant 1.10^{2}$ сек$^{-1}$.

Кроме того, дается сравнение между эффектом скорости деформации в испытаниях чистого сдвига, растяжения и сжатия. Это сравнеине дает возможность получить предварителные величины поведения скорости деформации двухосных напряженных состояний.

В конце концов, в свете этих испытаний исследуются основные предположения теории вязкопластичности для сложенных напряженных состояний.